VI. Conclusion and Future Work

This paper has discussed the new multicast scheduling strategies that jointly optimize the ARNC and SVC to maximize the average network throughput. The proposed ARNC is able to decode part of the original data when only a partial set of the RNC packets is received. Furthermore, the number of prioritized data layers is optimized to maximize the network throughput under different feedback assumptions. In the future, we will expand our work and consider user mobility, such as in [16].

References

[1] H. Schwarz, D. Marpe, and T. Wieg, "Overview of the scalable video coding extension of the H.264/AVC standard," *IEEE Trans. Circuits Syst. Video Technol.*, vol. 17, no. 9, pp. 1103–1120, Mar. 2007.

[2] Y. H. Moon, K. S. Yoon, S.-T. Park, and I. H. Shin, "A new fast encoding algorithm based on an efficient motion estimation process for the scalable video coding standard," *IEEE Trans. Multimedia*, vol. 15, no. 3, pp. 477–484, Apr. 2013.

[3] T. Tran, H. Li, W. Lin, L. Liu, and S. Khan, "Adaptive scheduling for multicasting hard deadline constrained prioritized data via network coding," in *Proc. IEEE GLOBECOM*, Dec. 2012, pp. 5843–5848.

[4] Z. Chen, T. J. Lim, and M. Motani, "Digital network coding aided two-way relaying: Energy minimization and queue analysis," *IEEE Trans. Wireless Commun.*, vol. 12, no. 4, pp. 1947–1957, Apr. 2013.

[5] C. Khirallah, D. Vukobratovic, and J. Thompson, "Performance analysis and energy efficiency of random network coding in LTE-advanced," *IEEE Trans. Wireless Commun.*, vol. 11, no. 12, pp. 4275–4285, Dec. 2012.

[6] T. Ho *et al.*, "A random linear network coding approach to multicast," *IEEE Trans. Inf. Theory*, vol. 52, no. 10, pp. 4413–4430, Oct. 2006.

[7] N. Dong, N. Thinh, and Y. Xue, "Joint network coding and scheduling for media streaming over multiuser wireless networks," *IEEE Trans. Veh. Technol.*, vol. 60, no. 3, pp. 1086–1098, Mar. 2011.

[8] Z. Kiraly and E. R. Kovacs, "A network coding algorithm for multi-layered video streaming," in *Proc. Int. Symp. NetCod*, Jul. 25–27, 2011, pp. 1–7.

[9] M. Xiao, M. Medard, and T. Aulin, "Cross-layer design of rateless random network codes for delay optimization," *IEEE Trans. Commun.*, vol. 59, no. 12, pp. 3311–3322, Dec. 2011.

[10] M. Dai, H. Y. Kwan, and C. W. Sung, "Linear network coding strategies for the multiple access relay channel with packet erasures," *IEEE Trans. Wireless Commun.*, vol. 12, no. 1, pp. 218–227, Jan. 2013.

[11] P. Wang, G. Mao, Z. Lin, and X. Ge, "An efficient network coding based broadcast scheme with reliability guarantee," in *Proc. IEEE ICC*, Jun. 2014, pp. 2873–2878.

[12] A. M. Sheikh, A. Fiandrotti, and E. Magli, "Distributed scheduling for low-delay and loss-resilient media streaming with network coding," *IEEE Trans. Multimedia*, vol. 16, no. 8, pp. 2294–2306, Dec. 2014.

[13] M. Wang and B. Li, "Network coding in live peer-to-peer streaming," *IEEE Trans. Multimedia*, vol. 9, no. 8, pp. 1554–1567, Dec. 2007.

[14] J. Krigslund, J. Hansen, M. Hundeboll, D. Lucani, and F. Fitzek, "CORE: COPE with MORE in wireless meshed networks," in *Proc. IEEE VTC Spring*, Jun. 2013, pp. 1–6.

[15] J. Wu, C. Yuen, B. Cheng, Y. Shang, and J. Chen, "Goodput-aware load distribution for real-time traffic over multipath networks," *IEEE Trans. Parallel Distrib. Syst.*, vol. 26, no. 8, pp. 2286–2299, Aug. 2015.

[16] J. Wu, B. Cheng, C. Yuen, Y. Shang, and J. Chen, "Distortion-aware concurrent multipath transfer for mobile video streaming in heterogeneous wireless networks," *IEEE Trans. Mobile Comput.*, vol. 14, no. 4, pp. 688–701, Apr. 2015.

Efficient Video Pricing and Caching in Heterogeneous Networks

Jun Li, *Member, IEEE*, Wen Chen, *Senior Member, IEEE*, Ming Xiao, *Senior Member, IEEE*, Feng Shu, *Member, IEEE*, and Xuan Liu

***Abstract*—Evidence indicates that downloading on-demand videos accounts for a dramatic increase in data traffic over cellular networks. Caching popular videos in the storage of small-cell base stations (SBSs), namely, small-cell caching, is an efficient technology for mitigating redundant data transmissions over backhaul channels in heterogeneous networks (HetNets). In this paper, we consider a commercialized small-cell caching system consisting of a video retailer (VR), multiple network service providers (NSPs), and mobile users (MUs). The VR leases its popular videos to the NSPs to make profits, and the NSPs, after placing these videos to their SBSs, can efficiently reduce the repetitive video transmissions over their backhaul channels. We study such a system within the framework of the Stackelberg game. We first model the MUs and SBSs as two independent Poisson point processes (PPPs) and develop the probability of the event that an MU can obtain the demanded video directly from the memory of an SBS. Then, based on the derived probability, we formulate a Stackelberg game to maximize jointly the average profit of the VR and the NSPs. Moreover, we investigate the Stackelberg equilibrium (SE) via solving an optimization problem. Numerical results are provided for verifying the proposed framework by showing its effectiveness on pricing and resource allocation.**

***Index Terms*—Heterogenous cellular networks, Stackelberg game, stochastic geometry, wireless caching.**

I. Introduction

Wireless data traffic is expected to increase exponentially in the next few years, driven by a dramatic growth of mobile users (MUs). There is evidence that MUs' downloading or streaming of on-demand videos is the major reason for the boost of data traffic over cellular networks [1].

Manuscript received June 2, 2015; revised December 10, 2015; accepted December 13, 2015. Date of publication December 24, 2015; date of current version October 13, 2016. This work was supported in part by the National Natural Science Foundation of China under Grant 61501238, Grant 61271230, Grant 61472190, and Grant 61371105; by the Jiangsu Provincial Science Foundation under Project BK20150786; by the Specially Appointed Professor Program in Jiangsu Province 2015; by the National 973 Program under Grant 2013CB329001; by the Open Research Fund of the National Key Laboratory of Electromagnetic Environment under Grant 201500013; by the Open Research Fund of the National Mobile Communications Research Laboratory, Southeast University, under Grant 2013D02; and by the EU Marie Curie Project QUICK. The review of this paper was coordinated by Prof. A. L. Grieco.

J. Li is with the School of Electronic and Optical Engineering, Nanjing University of Science and Technology, Nanjing 210094, China (e-mail: jun.li@njust.edu.cn).

W. Chen is with the Department of Electronic Engineering, Shanghai Jiao Tong University, Shanghai 200240, China (e-mail: wenchen@sjtu.edu.cn).

M. Xiao is with the School of Electrical Engineering, Royal Institute of Technology, 100 44 Stockholm, Sweden (e-mail: ming.xiao@ee.kth.se).

F. Shu is with the School of Electronic and Optical Engineering, Nanjing University of Science and Technology, Nanjing 210094, China, with the National Key Laboratory of Electromagnetic Environment, China Research Institute of Radiowave Propagation, Beijing 266107, China, and also with the National Mobile Communications Research Laboratory, Southeast University, Nanjing 210096, China (e-mail: shufeng@njust.edu.cn).

X. Liu is with the School of Electrical and Information Engineering, University of Sydney, Sydney, NSW 2006, Australia (e-mail: xuan.liu@sydney.edu.au).

Color versions of one or more of the figures in this paper are available online at http://ieeexplore.ieee.org.

Digital Object Identifier 10.1109/TVT.2015.2511806

It is observed that numerous repetitive requests of popular videos from the MU's account are for redundant video streaming. The redundancy of data transmissions can be reduced by locally storing popular videos, known as caching, into the storage of intermediate network nodes [1], [2].

Generally, wireless data caching consists of two stages: data placement and data delivery. In the data placement stage, popular videos are cached into local storage during off-peak time, whereas in the data delivery stage, requested videos are delivered from the local caching system to the MUs. Recent works advance the caching technology in device-to-device networks and wireless sensor networks [3]–[5].

As small-cell embedded architectures prevail in future cellular networks, known as heterogeneous networks (HetNets) [6], [7], the reliance of caching on small-cell base stations (SBS), namely small-cell caching, is a promising trend. The advantages brought by the small-cell caching are threefold. First, popular videos are pushed closer to the MUs when cached in SBSs, reducing the transmission latency. Second, redundant data transmissions over SBSs' backhaul channels are mitigated, which are usually expensive [8]. Third, the majority of video traffic is offloaded from macrocell base stations to SBSs. In [9], a small-cell caching scheme, named "Femtocaching," is proposed for a cellular network embedded with SBSs, where the data placement at the SBSs is optimized in a centralized manner for reducing the transmission delay imposed. In [10], the small-cell caching is investigated in the context of stochastic networks. The average performance is developed via stochastic geometry [11], [12], where the distribution of network nodes are modeled by a Poisson point process (PPP).

From the above discussions, current research on wireless caching mainly considers the data placement issue for reducing download delay. However, the whole caching system is coupled with many issues other than data placement. From a commercial perspective, it will be more interesting to consider the topics such as pricing on video downloading, rental of local storage, and so on. A commercialized caching system may consist of video retailers (VRs), network service providers (NSPs), and MUs. The VRs purchase copyrights from video producers and publish the videos on their websites. The NSPs are typically operators of cellular networks who are in charge of network facilities, such as macrocell base stations and SBSs.

In such a commercialized small-cell caching system, to reduce the repetitive video transmissions over backhaul channels, the NSPs are willing to pay for renting some popular videos from the VRs, and then cache the copies of these videos to their SBSs. The profits gained by the NSPs are from the saved costs on backhaul channels. At the same time, since the VRs lease their videos to the NSPs, they can make profits as well. For a given leasing price, the more video copies the VRs lease to the NSPs, the more profit they will gain. In this sense, both the VRs and NSPs are the beneficiaries from the local caching system. However, each entity is selfish and wishes to maximize its own benefit. For instance, the NSPs are trying to negotiate with the VRs for a low price on renting a video, whereas the VRs want a higher price. This will raise a competition and optimization problem on bargaining the price, which can be effectively solved within the framework of game theory. We note that game theory has been successfully applied to wireless communications for solving resource allocation problems [13]–[18].

In this paper, we consider a commercialized small-cell caching system that consists of a VR and multiple NSPs and MUs, and optimize such a system within the framework of a Stackelberg game. Generally speaking, a Stackelberg game is a strategic game that consists of a leader and a follower [17], where the leader moves first and the follower moves subsequently. Correspondingly, in our game-theoretic caching system, we consider the VR as a leader and the NSPs as the followers. The VR sets prices for leasing copies of its videos, whereas the NSPs optimize how many copies they need to rent. In particular, our contributions are as follows.

1) We model the MUs and SBSs in the network as two different ties of a Poisson point process [12]. Under this network model, we develop the probability of the event that an MU can obtain the demanded video directly from the storage of an SBS.
2) Based on the derived probability, we develop the profit model for the caching system and formulate the profits gained by the VR and the NSPs.
3) A Stackelberg game is proposed for jointly maximizing the average profit of the VR and the NSPs, and its Stackelberg equilibrium (SE) is also investigated.

The remainder of this paper is organized as follows. We describe the system model in Section II and discuss the caching process in Section III. We then establish the profit model and formulate the Stackelberg game for the caching system in Section IV. The system is optimized, and the SE is investigated in Section V. Our numerical results are provided in Section VI, and our conclusions are summarized in Section VII.

II. System Model

We consider a commercialized small-cell caching system consisting of a VR, L NSPs, and multiple MUs, where each NSP is in charge of a set of SBSs. $\mathcal{V}$ denotes the VR, $\boldsymbol{\mathcal{L}} \triangleq \{\mathcal{L}_1, \mathcal{L}_2, \ldots, \mathcal{L}_L\}$ denotes the set of the NSPs, and $\mathcal{M}$ denotes one of the MUs. In such a system, the NSPs wish to rent the copies of popular videos from $\mathcal{V}$ and cache these videos into the storage of their SBSs. Due to the local caching, the NSPs can offer fast video downloading to the MUs and reduce the usage of the NSPs' backhaul channels. At the same time, the VR makes profit by renting these videos. Both the VR and each NSP try to maximize their profits.

There are three stages in the system. In the first stage, the VR purchases the copyrights of popular videos from video producers and publishes them on its website. In the second stage, the NSPs negotiate with the VR on renting the copies of these popular videos. Upon obtaining these videos, each NSP will place them in the storage of its SBSs. In the third stage, the MUs connect to the SBSs to download desired videos. We will particularly focus on the second and third stages within the game-theoretic framework.

A. Network Model

Let us consider a small-cell based caching network composed of the MUs and the SBSs owned by $\boldsymbol{\mathcal{L}}$, where all the SBSs are deployed with a unified transmit power P and transmit on the same channel. Moreover, assume that all the SBSs transmit on the channels orthogonal to those of the macrocell base stations; thus, there is no interference incurred by the macrocell base stations. Assume that the SBSs owned by $\mathcal{L}_l$, $l = 1, \ldots, L$ are spatially distributed as a homogeneous PPP (HPPP) Φ_l of intensity λ_l. Here, the intensity λ_l represents the number of SBSs of $\mathcal{L}_l$ in per unit area. To simplify the notation, the PPP Φ_l is also used to represent the set of points in this process. Furthermore, we model the distribution of the MUs that belong to the NSP $\mathcal{L}_l$ as an independent HPPP Ψ_l of intensity $\zeta_l \; \forall \, l$.

The wireless downlink channels spanning from the SBSs to the MUs are independent and identically distributed, and modeled as the combination of path loss and Rayleigh fading. Without loss of generality, we conduct our analysis on a typical MU of $\mathcal{L}_l$ located at the origin. The path loss between an SBS located at x and the typical MU is denoted by $\|x\|^{-\alpha}$, where α is the path-loss exponent. The channel power of the Rayleigh fading between them is denoted by h_x, where $h_x \sim \exp(1)$. The noise at each MU is Gaussian distributed with variance σ^2.

We consider a saturate network, where all the SBSs are powered on and keep transmitting data for serving their MUs. Hence, the received signal-to-interference-plus-noise ratio (SINR) at the typical MU from an SBS of $\mathcal{L}_l$, which is located at x_l, can be expressed as

$$\rho(x_l)=\frac{Ph_{x_l}\|x_l\|^{-\alpha}}{\sum_{l'\neq l}\sum_{x\in\Phi_{l'}}Ph_x\|x\|^{-\alpha}+\sum_{x\in\Phi_l\setminus x_l}Ph_x\|x\|^{-\alpha}+\sigma^2} \quad (1)$$

where the numerator $Ph_{x_l}\|x_l\|^{-\alpha}$ represents the received signal power at the origin from the SBS located at x_l. The first item in the denominator, i.e., $\sum_{l'\neq l}\sum_{x\in\Phi_{l'}}Ph_x\|x\|^{-\alpha}$ is the sum interference caused by the SBSs from the NSPs other than $\mathcal{L}_l$. The second item in the denominator, i.e., $\sum_{x\in\Phi_l\setminus x_l}Ph_x\|x\|^{-\alpha}$ is the sum interference caused by the SBSs from $\mathcal{L}_l$ except for the SBS located at x_l. The typical MU is considered "covered" by an SBS located at x_l as long as $\rho(x_l)$ is no less than a preset SINR threshold δ, i.e., $\rho(x_l)\geq\delta$.

B. Video Popularity

We now model the popularity distribution, i.e., the distribution of request probabilities, among the popular videos to be cached. Denote by $\boldsymbol{\mathcal{F}}=\{\mathcal{F}_1,\mathcal{F}_2,\ldots,\mathcal{F}_F\}$ the file set consisting of F video files. The popularity distribution among $\boldsymbol{\mathcal{F}}$ is represented by a vector $\mathbf{p}=[p_1,p_2,\ldots,p_F]$. That is, the MUs make independent requests of the fth video $\mathcal{F}_f$, $f=1,\ldots,F$, with the probability of p_f. Generally, $\mathbf{p}$ can be modeled by the Zipf popularity distribution [19] as

$$p_f=\frac{\frac{1}{f^\beta}}{\sum_{j=1}^{F}\frac{1}{j^\beta}},\quad \forall f \quad (2)$$

where the exponent β is a positive value, characterizing the video popularity. A larger β corresponds to a higher content reuse, i.e., the most popular files account for the majority of requests. Moreover, from (2), the file with a smaller f corresponds to a larger popularity.

III. Small-Cell Caching Process

Here, we introduce the process of our small-cell caching system. In the first stage, the VR purchases the F popular videos in $\boldsymbol{\mathcal{F}}$ from the producers and publishes these videos on its website. In the second stage, the NSPs negotiate with the VR for renting these videos. As the storage is generally cheap, we assume that each SBS has a large enough storage for caching all the F videos. However, caching a video at an SBS will depend on whether the NSPs can make a profit from renting this video. Obviously, the NSPs will choose not to rent a video if its price is too high such that no profit can be gained.

Moreover, in the second stage, we consider a random caching strategy. In this strategy, each NSP randomly chooses a fraction of its SBSs for caching a specific video. In particular, $\tau_{l,f}$ denotes the fraction of the SBSs owned by $\mathcal{L}_l$ that are selected for caching $\mathcal{F}_f$, where each of these SBSs caches one copy of $\mathcal{F}_f$. We have $0\leq\tau_{l,f}\leq 1$, where $\tau_{l,f}=1$ represents that $\mathcal{L}_l$ places the video $\mathcal{F}_f$ into each of its SBSs, whereas $\tau_{l,f}=0$ represents that $\mathcal{L}_l$ does not cache $\mathcal{F}_f$ at all. As we will discuss in the following, $\tau_{l,f}$ should be optimized to maximize $\mathcal{L}_l$'s profit. Since the SBSs are randomly picked for caching a video, we can thus model the distribution of the SBSs owned by $\mathcal{L}_l$ that cache the video $\mathcal{F}_f$ as a "thinned" HPPP $\Phi_{l,f}$, with intensity $\tau_{l,f}\lambda_l$.

In the third stage, the MUs start to download videos. When an MU $\mathcal{M}$ of $\mathcal{L}_l$, i.e., $\mathcal{M}\in\Psi_l$, demands a video $\mathcal{F}_f$, it searches the SBSs in $\Phi_{l,f}$ and tries to connect to the nearest SBS that covers $\mathcal{M}$. In the case that such an SBS exists, the MU $\mathcal{M}$ will obtain this video directly from the storage of this SBS, and we thereby define such an event by $\mathcal{E}_{l,f}$. In the case that such an SBS does not exist, $\mathcal{M}$ will be redirected to the central server of $\mathcal{V}$ for downloading the requested file $\mathcal{F}_f$. As the server of $\mathcal{V}$ is located at the backbone network, this redirection of the demand will trigger a transmission via the backhaul channels of the NSP $\mathcal{L}_l$, leading to an extra cost.

Under the PPP distribution of the network nodes, we now derive the probability $\Pr(\mathcal{E}_{l,f})$ of the event $\mathcal{E}_{l,f}$ $\forall\, l,f$, in the following theorem.

Theorem 1: The probability of the event $\mathcal{E}_{l,f}$ can be expressed as

$$\Pr(\mathcal{E}_{l,f})=\frac{\tau_{l,f}\lambda_l}{C(\delta,\alpha)\left(\sum_{j=1}^{L}\lambda_j-\tau_{l,f}\lambda_l\right)+A(\delta,\alpha)\tau_{l,f}\lambda_l+\tau_{l,f}\lambda_l} \quad (3)$$

where $A(\delta,\alpha)\triangleq(2\delta/\alpha-2)\ {}_2F_1(1,1-(2/\alpha);2-(2/\alpha);-\delta)$ and $C(\delta,\alpha)\triangleq(2/\alpha)\delta^{2/\alpha}B(2/\alpha,1-(2/\alpha))$. ${}_2F_1(\cdot)$ in the function $A(\delta,\alpha)$ is the hypergeometric function, and the beta function in $C(\delta,\alpha)$ is formulated as $B(z,y)=\int_0^1 t^{z-1}(1-t)^{y-1}\mathrm{d}t$.

Proof: See Appendix A. ∎

From (3), we can see that, due to the assumption that the SBSs' cochannel transmissions with the same power, $\Pr(\mathcal{E}_{l,f})$ is independent of the transmission power P of the SBSs.

Remark 1: In *Theorem 1*, increasing $\tau_{l,f}$ can increase the probability $\Pr(\mathcal{E}_{l,f})$ to some degree. However, from (3) in the theorem, it is not efficient to always increase $\tau_{l,f}$ to obtain a higher $\Pr(\mathcal{E}_{l,f})$. This property will provide us a chance to find the equilibrium in the game described in the following.

IV. Problem Formulation

Here, we first model the profit gained by the VR and the NSPs. Then, we formulate the profit-maximization problem within the framework of a Stackelberg game.

A. Profit Modeling

We focus on modeling the profit of the VR and the NSPs obtained from the small-cell caching system. Average profit is developed based on stochastically geometrical distributions of the network nodes in terms of per unit area and per unit period (/UAP), e.g., /month $\cdot$ km^2.

We first model the profit at the NSP side and consider the NSP $\mathcal{L}_l$ without loss of generality. The revenue gained by $\mathcal{L}_l$ is from the saved cost of backhaul channels due to local caching. Once an MU downloads a required video from the local storage, the NSP can save a video transmission over backhaul channels. Therefore, we have the saved cost/UAP of $\mathcal{L}_l$ as

$$S_l^{\mathrm{BH}}=\sum_{j=1}^{F}p_j\zeta_l K\Pr(\mathcal{E}_{l,j})s^{\mathrm{bh}} \quad (4)$$

where K represents the average number of video demands from each MU within a unit period, and s^{bh} is the average backhaul cost for a video transmission. Note that in [20], monthly costs on renting backhaul channels are investigated, which can quantify the value of s^{bh} for a video transmission via a backhaul channel in real systems.

At the same time, $\mathcal{L}_l$ pays for renting the videos from $\mathcal{V}$. We assume that the VR will charge a price $s_{l,f}$ $\forall\, f$, on $\mathcal{L}_l$'s renting a copy of $\mathcal{F}_f$ during a unit period. Since there are, on average, $\tau_{l,f}\lambda_l$ SBSs caching $\mathcal{F}_f$, the average cost/UAP of $\mathcal{L}_l$ on renting videos can be calculated as

$$S_l^{\mathrm{RT}}=\sum_{j=1}^{F}\tau_{l,j}\lambda_l s_{l,j}. \quad (5)$$

Combining the given two items, the overall profit/UAP for $\mathcal{L}_l$ can be expressed as

$$S_l^{\mathrm{NSP}}=S_l^{\mathrm{BH}}-S_l^{\mathrm{RT}}. \quad (6)$$

For the VR, its profit comes directly from leasing the video copies, which can be written as

$$S^{\mathrm{VR}} = \sum_{j_1=1}^{L} \sum_{j_2=1}^{F} \tau_{j_1,j_2} \lambda_{j_1} s_{j_1,j_2}. \tag{7}$$

B. Stackelberg Game Formulation

The Stackelberg game is a strategic game that consists of a leader and several followers competing for certain resources [17]. The leader moves first, and the followers move subsequently. In our small-cell caching system, we model the VR $\mathcal{V}$ as the leader, and the L NSPs as the followers. The VR imposes a price vector $\mathbf{s}_l = [s_{l,1}, s_{l,2}, \ldots, s_{l,F}]$ on the NSP $\mathcal{L}_l \, \forall \, l$, where $s_{l,f} \, \forall \, f$, has been defined as the price charged for $\mathcal{L}_l$'s renting a copy of $\mathcal{F}_f$ per unit period. After the price vector $\mathbf{s}$ is set, the NSP $\mathcal{L}_l \, \forall \, l$, updates $\boldsymbol{\tau}_l \triangleq [\tau_{l,1}, \ldots, \tau_{l,F}]$ for maximizing its profit.

1) Optimization Formulation of the Leader: From the given game model, we observe that the VR's objective is to maximize its profit S^{VR} in (7). Note that the fraction $\tau_{l,f}$ is a function of the price $s_{l,f}$ under the Stackelberg game formulation. This means that the number of copies of the file $\mathcal{F}_f$ that each NSP is willing to rent depends on the price. Consequently, the VR needs to find the optimal price vector $\mathbf{s}_l \, \forall \, l$, to maximize its profit. This optimization problem can be summarized as follows.

Problem 1: The optimization problem on maximizing $\mathcal{V}$'s profit can be written as

$$\max_{\mathbf{s}_1,\ldots,\mathbf{s}_L} S^{\mathrm{VR}}(\mathbf{s}_1, \ldots, \mathbf{s}_L, \boldsymbol{\tau}_1, \ldots, \boldsymbol{\tau}_L), \quad \text{s.t. } 0 \le \tau_{l,f} \le 1 \quad \forall \, l, f. \tag{8}$$

2) Optimization Formulation of the Followers: The profit gained by the NSP $\mathcal{L}_l$ in (6) can be further written as (9), shown at the bottom of the page. We can see from (9) that once the price vector $\mathbf{s}_l$ is fixed, the profit of $\mathcal{L}_l$ depends on $\tau_{l,f} \, \forall \, f$. Therefore, $\tau_{l,f}$ needs to be optimized for maximizing the profit of $\mathcal{L}_l$. Mathematically, this optimization can be formulated as follows.

Problem 2: The optimization problem on maximizing $\mathcal{L}_l$'s profit can be written as

$$\max_{\boldsymbol{\tau}_l} S_l^{\mathrm{NSP}}(\boldsymbol{\tau}_l, \mathbf{s}_l), \quad \text{s.t. } 0 \le \tau_{l,f} \le 1 \quad \forall \, l, f. \tag{10}$$

Problems 1 and 2 together form a Stackelberg game. The objective is to find the SE points from which neither the leader (VR) nor the followers (NSPs) have incentives to deviate. In the following, we investigate the Stackelberg Equilibrium (SE) points for the proposed game.

3) Stackelberg Equilibrium: For our Stackelberg game, the SE is defined as follows.

Definition 1: Let $\mathbf{s}_l^\star \triangleq [s_{l,1}^\star, s_{l,2}^\star, \ldots, s_{l,F}^\star]$ be a solution for Problem 1, and $\boldsymbol{\tau}_l^\star \triangleq [\tau_{l,1}^\star, \tau_{l,2}^\star, \ldots, \tau_{l,F}^\star]$ be a solution for Problem 2, $\forall \, l$. Then $(\mathbf{s}_1^\star, \ldots, \mathbf{s}_L^\star, \boldsymbol{\tau}_1^\star, \ldots, \boldsymbol{\tau}_L^\star)$ is an SE for the proposed Stackelberg game if for any $(\mathbf{s}_1, \ldots, \mathbf{s}_L, \boldsymbol{\tau}_1, \ldots, \boldsymbol{\tau}_L)$, the following conditions hold:

$$S^{\mathrm{VR}}(\mathbf{s}_1^\star, \ldots, \mathbf{s}_L^\star, \boldsymbol{\tau}_1^\star, \ldots, \boldsymbol{\tau}_L^\star) \ge S^{\mathrm{VR}}(\mathbf{s}_1, \ldots, \mathbf{s}_L, \boldsymbol{\tau}_1^\star, \ldots, \boldsymbol{\tau}_L^\star),$$
$$S_l^{\mathrm{NSP}}(\boldsymbol{\tau}_l^\star, \mathbf{s}_l^\star) \ge S_l^{\mathrm{NSP}}(\boldsymbol{\tau}_l, \mathbf{s}_l^\star) \quad \forall \, l. \tag{11}$$

Therefore in our game, we first solve Problem 2, given the price vectors $\mathbf{s}_l \, \forall \, l$. Then, with the obtained best response function $\boldsymbol{\tau}_l^\star$ of the NSP $\mathcal{L}_l$, we solve Problem 1 for the optimal price $\mathbf{s}_l^\star$. We note that in [14], the followers' bounded rationality and limited observation of the leader's strategy are discussed, which may lead to deviations of the followers' expected optimal response. However, since, in this paper, both the followers (NSPs) and the leader (VR) are not located in the wireless networks, they can exchange information via robust communication approaches, such as wire-line networks. Therefore, in this paper, it is reasonable to assume that the followers are capable of accurately tracking the leader's strategy. In the following, we will investigate in-depth the game-theoretic optimization.

V. Game-Theoretic Optimization

Here, we will solve the optimization problem in our game. We first solve Problem 2 at the NSPs, and we observe that (9) is a concave function over the variable $\tau_{l,f}$. Thus, by solving the Karush–Kuhn–Tucker (KKT) conditions, we have an optimal solution for Problem 2 as

$$\tau_{l,f}^\star = \left(\frac{1}{(A+1-C)\lambda_l} \sqrt{\frac{p_f \zeta_l K s^{\mathrm{bh}} C \sum_{j=1}^{L} \lambda_j}{s_{l,f}}} - \frac{C \sum_{j=1}^{L} \lambda_j}{(A+1-C)\lambda_l} \right)^{\pm} \tag{12}$$

where $(x)^{\pm}$ represents $0 \le x \le 1$, and A and C represent the functions $A(\delta, \alpha)$ and $C(\delta, \alpha)$, respectively, for simplicity.

We can see that, if the price $s_{l,f}$ is too low, i.e.,

$$s_{l,f} < s_{l,f}^{\mathrm{lower}} \triangleq \frac{p_f \zeta_l K s^{\mathrm{bh}} C \sum_{j=1}^{L} \lambda_j}{\left(C \sum_{j=1}^{L} \lambda_j + (A+1-C)\lambda_l \right)^2} \tag{13}$$

which implies $\tau_{l,f} > 1$, then $\mathcal{L}_l$ will rent the maximum number of copies of $\mathcal{F}_f$ to make sure that each of its SBSs caches one copy. On the other hand, if $s_{l,f}$ is too high, i.e.,

$$s_{l,f} > s_{l,f}^{\mathrm{upper}} \triangleq \frac{p_f \zeta_l K s^{\mathrm{bh}}}{C \sum_{j=1}^{L} \lambda_j} \tag{14}$$

which implies $\tau_{l,f} < 0$, then $\mathcal{L}_l$ will choose not to rent $\mathcal{F}_f$. Hence, a reasonable price of $s_{l,f}$ should satisfy $s_{l,f}^{\mathrm{lower}} \le s_{l,f} \le s_{l,f}^{\mathrm{upper}}$.

$$\begin{aligned} S_l^{\mathrm{NSP}}(\boldsymbol{\tau}_l, \mathbf{s}_l) &= \sum_{j=1}^{F} \left(p_j \zeta_l K \Pr(\mathcal{E}_{l,j}) s^{\mathrm{bh}} - \tau_{l,j} \lambda_l s_{l,j} \right) \\ &= \sum_{j=1}^{F} \left(-\tau_{l,j} \lambda_l s_{l,j} + \frac{p_j \zeta_l K s^{\mathrm{bh}} \tau_{l,j} \lambda_l}{C(\delta,\alpha) \left(\sum_{i=1}^{L} \lambda_i - \tau_{l,j} \lambda_l \right) + A(\delta,\alpha) \tau_{l,j} \lambda_l + \tau_{l,j} \lambda_l} \right). \end{aligned} \tag{9}$$

Substituting the optimal $\tau^{\star}_{l,f}$ of (12) into (7) with some manipulations, we have

$$S^{\mathrm{VR}} = \sum_{j_1=1}^{L}\sum_{j_2=1}^{F} -\frac{C\sum_{j=1}^{L}\lambda_j}{A+1-C}s_{j_1,j_2} + \frac{\sqrt{s_{j_1,j_2}}}{A+1-C}\sqrt{p_{j_2}\zeta_{j_1}Ks^{\mathrm{bh}}C\sum_{j=1}^{L}\lambda_j} = \sum_{j_1=1}^{L}\sum_{j_2=1}^{F}\frac{p_{j_2}\zeta_{j_1}KS^{\mathrm{bh}}}{4(A+1-C)} - \frac{C\sum_{j=1}^{L}\lambda_j}{A+1-C}\left(\sqrt{s_{j_1,j_2}} - \frac{1}{2}\sqrt{\frac{p_{j_2}\zeta_{j_1}KS^{\mathrm{bh}}}{C\sum_{j=1}^{L}\lambda_j}}\right)^2. \quad (15)$$

From (15), the price of $\mathcal{F}_f$ on $\mathcal{L}_l$ that maximizes S^{VR} without constraint is $s'_{l,f} \triangleq (1/4)((p_f\zeta_l Ks^{\mathrm{bh}})/(C\sum_{j=1}^{L}\lambda_j))$. Considering the constraint $s^{\mathrm{lower}}_{l,f} \le s_{l,f} \le s^{\mathrm{upper}}_{l,f}$, the optimal price $s^{\star}_{l,f}$ is obtained by comparing $s'_{l,f}$ with the two bounds. We have three cases: 1) If $s'_{l,f} > s^{\mathrm{upper}}_{l,f}$, then we have $s^{\star}_{l,f} = s^{\mathrm{upper}}_{l,f}$; 2) if $s^{\mathrm{lower}}_{l,f} \le s'_{l,f} \le s^{\mathrm{upper}}_{l,f}$, then we have $s^{\star}_{l,f} = s'_{l,f}$; 3) If $s'_{l,f} < s^{\mathrm{lower}}_{l,f}$, then we have $s^{\star}_{l,f} = s^{\mathrm{lower}}_{l,f}$.

In the first case, we observe that $s'_{l,f}$ is always less than $s^{\mathrm{upper}}_{l,f}$. Hence, this case will not be considered. In the second case, to ensure $s'_{l,f} \ge s^{\mathrm{lower}}_{l,f}$, the requirement on λ_l is

$$\lambda_l \ge \lambda^{\mathrm{thr}} \triangleq \frac{C}{A+1-C}\sum_{j=1}^{L}\lambda_j. \quad (16)$$

From the given discussions, we conclude that the optimal price for $\mathcal{L}_l$'s renting a copy of $\mathcal{F}_f$ as

$$s^{\star}_{l,f} = \begin{cases} \frac{1}{4}\frac{p_f\zeta_l Ks^{\mathrm{bh}}}{C\sum_{j=1}^{L}\lambda_j}, & \text{if } \lambda_l \ge \lambda^{\mathrm{thr}} \\ \frac{p_f\zeta_l Ks^{\mathrm{bh}}C\sum_{j=1}^{L}\lambda_j}{\left(C\sum_{j=1}^{L}\lambda_j+(A+1-C)\lambda_l\right)^2}, & \text{otherwise.} \end{cases} \quad (17)$$

Remark 2: The optimal price $s^{\star}_{l,f}$ charged for $\mathcal{L}_l$ for renting a copy of $\mathcal{F}_f$ is always proportional to p_f, ζ_l, K, and s^{bh}.

Remark 3: Given the intensities $\lambda_1, \ldots, \lambda_L$, if λ_l is larger than the threshold λ^{thr}, the optimal price for $\mathcal{L}_l$ for renting a copy of $\mathcal{F}_f \ \forall f$, is independent of λ_l.

Furthermore, plugging $s^{\star}_{l,f}$ into (12), we have

$$\tau^{\star}_{l,f} = \begin{cases} \frac{C\sum_{j=1}^{L}\lambda_j}{(A+1-C)\lambda_l}, & \text{if } \lambda_l \ge \lambda^{\mathrm{thr}} \\ 1, & \text{otherwise.} \end{cases} \quad (18)$$

Remark 4: Given the intensities $\lambda_1, \ldots, \lambda_L$, if λ_l is larger than the threshold λ^{thr}, the NSP $\mathcal{L}_l$ should rent a fixed number $\tau^{\star}_{l,f}\lambda_l = (C\sum_{j=1}^{L}\lambda_j)/(A+1-C)$ of the copies of $\mathcal{F}_f \ \forall f$, per unit area. Otherwise, $\mathcal{L}_l$ should rent λ_l copies of $\mathcal{F}_f \ \forall f$, per unit area, i.e., each SBS caches one copy of $\mathcal{F}_f$.

VI. Numerical Results

Here, we provide numerical results to evaluate the performances of the proposed framework. We set the path-loss exponent to $\alpha = 4$ and set the number of files in $\boldsymbol{\mathcal{F}}$ to $F = 500$. Moreover, we consider $L = 4$ NSPs, $\mathcal{L}_1$, $\mathcal{L}_2$, $\mathcal{L}_3$, and $\mathcal{L}_4$, with intensities $\lambda_1 = 5/\mathrm{km}^2$, $\lambda_2 = 10/\mathrm{km}^2$, $\lambda_3 = 50/\mathrm{km}^2$, and $\lambda_4 = 100/\mathrm{km}^2$. For the pricing system, the profit/UAP is consider to be the profit gained per month within an area of 1 km^2, i.e., /month $\cdot$ km^2. We note that the profits gained by the VR and by the NSPs are proportional to s^{bh}. Hence, without loss of generality, we set $s^{\mathrm{bh}} = 1$, for simplicity. In addition, we set $K = 10$/month, which is the average number of video requests from an MU per month.

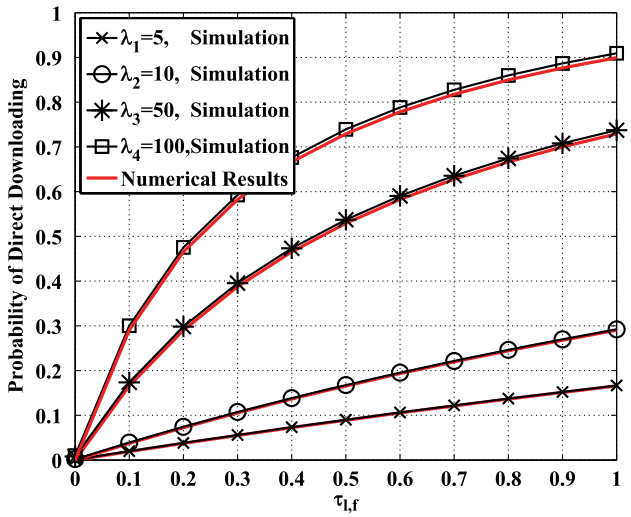

Fig. 1. Comparisons between the simulations and analytical results on $\Pr(\mathcal{E}_{l,f})$ versus various values of $\tau_{l,f}$.

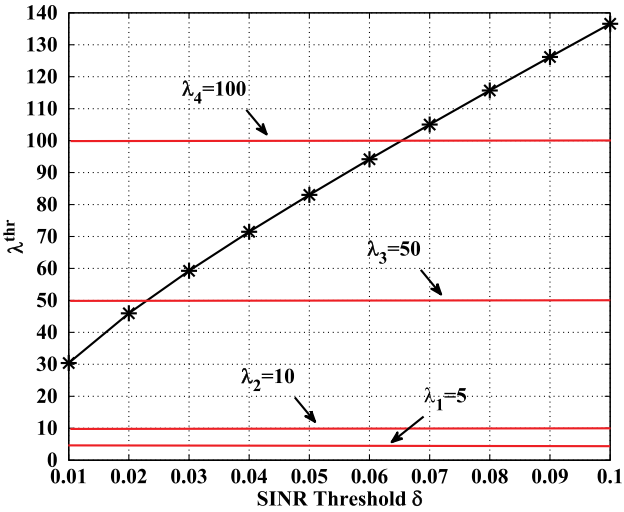

Fig. 2. Value of λ^{thr} under various values of the SINR threshold δ.

We begin with verifying $\Pr(\mathcal{E}_{l,f})$ in *Theorem 1* by comparing the numerical result with Monte Carlo simulations. In the simulations, all the average performances are evaluated over a thousand network cases, where the distributions of the SBSs and the MUs change from case to case according to the PPPs Φ_l and $\Psi_l \ \forall l$, respectively. We can see from the expression of $\Pr(\mathcal{E}_{l,f})$ that it is a function of $\tau_{l,f}$. Although $\tau_{l,f}$ should be optimized according to the price charged by the NSP, here, we set a variety of $\tau_{l,f}$ values, from 0 to 1, to verify the trend of $\Pr(\mathcal{E}_{l,f})$. Fig. 1 shows the comparisons between the simulations and analytical results on $\Pr(\mathcal{E}_{l,f})$, $l = 1, 2, 3, 4$, under various $\tau_{l,f}$ and $\delta = 0.01$. We can see that the simulations results match the analytical results derived in *Theorem 1*. Moreover, a larger intensity leads to a higher direct download probability.

After verifying the behavior on $\Pr(\mathcal{E}_{l,f})$, we now provide numerical results of our Stackelberg framework. We first investigate the value of λ^{thr} under different values of the SINR threshold δ from 0.01 to 0.1. In Fig. 2, we can see that λ^{thr} is an increasing function of δ. Moreover, λ_1 and λ_2 are always below the value of λ^{thr}. According to (18), this means that $\tau_{1,f} = \tau_{2,f} = 1$, i.e., $\mathcal{L}_1$ and $\mathcal{L}_2$ need to always cache a copy of $\mathcal{F}_f \ \forall f$, in each of their SBSs. For $\mathcal{L}_3$, when $\delta < 0.023$, we have $\lambda_3 > \lambda^{\mathrm{thr}}$. Therefore, $\mathcal{L}_3$ should randomly choose a fraction

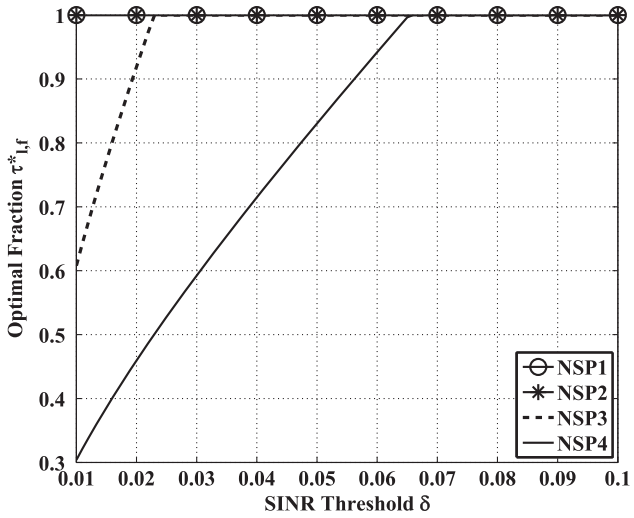

Fig. 3. Value of $\tau^{\star}_{l,f}$ under various values of the SINR threshold δ for the four NSPs.

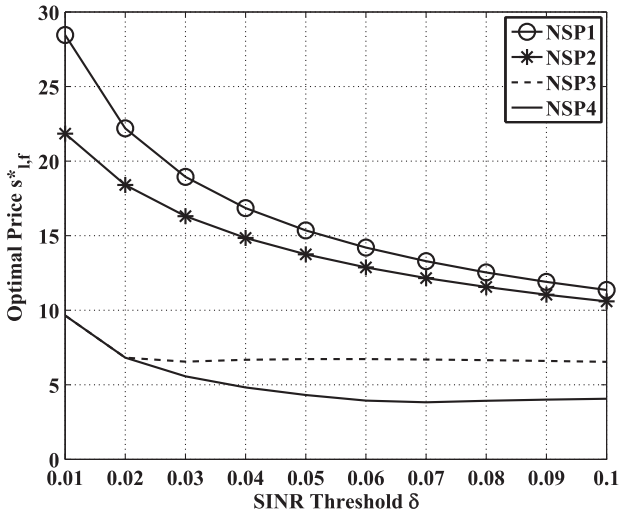

Fig. 4. Value of $s^{\star}_{l,f}$ under various values of the SINR threshold δ for the four NSPs.

$\tau_{3,f} = ((C\sum_{j=1}^{L}\lambda_j)/(A+1-C))\lambda_l < 1$ of its SBSs for caching the file $\mathcal{F}_f$, whereas when $\delta \geq 0.023$, i.e., $\lambda_3 \leq \lambda^{\rm thr}$, $\mathcal{L}_3$ needs to cache $\mathcal{F}_f$ in each of its SBSs $\forall f$. Similarly, for $\mathcal{L}_4$, when $\delta \geq 0.065$, i.e., $\lambda_4 \leq \lambda^{\rm thr}$, it caches $\mathcal{F}_f$ in all of its SBSs, whereas when $\delta < 0.065$, only a fraction $\tau_{4,f} < 1$ of its SBSs need to cache $\mathcal{F}_f$ $\forall f$. Fig. 3 further shows the optimal fraction $\tau^{\star}_{l,f}$ under different values of δ, where NSP1, NSP2, NSP3, and NSP4 in the legend represent $\mathcal{L}_1, \mathcal{L}_2, \mathcal{L}_3$, and $\mathcal{L}_4$, respectively. We can see that both $\tau^{\star}_{3,f}$ and $\tau^{\star}_{4,f}$ increase with δ before they reach 1.

Then, we investigate the optimal price $s^{\star}_{l,f}$ in (17) under different values of δ for the four NSPs. To have a better comparison, we consider a specific value of $p_f = 0.5$, and set $\zeta_1 = \zeta_2 = \zeta_3 = \zeta_4 = 200$. Fig. 4 shows the optimal price for the four NSPs under different δ. It is interesting to observe that a higher price will be charged on the NSP with less dense SBSs. It is, however, reasonable from the VR's viewpoint since the NSP with less SBSs will rent less video copies from the VR. Thus, the price for a video copy has to be raised to maximize the VR's profit. Note that there is an overlap for the prices of $\mathcal{L}_3$ and $\mathcal{L}_4$ when $\delta < 0.023$. This is because both λ_3 and λ_4 are larger than $\lambda^{\rm thr}$ when $\delta < 0.023$, and the optimal prices for the two

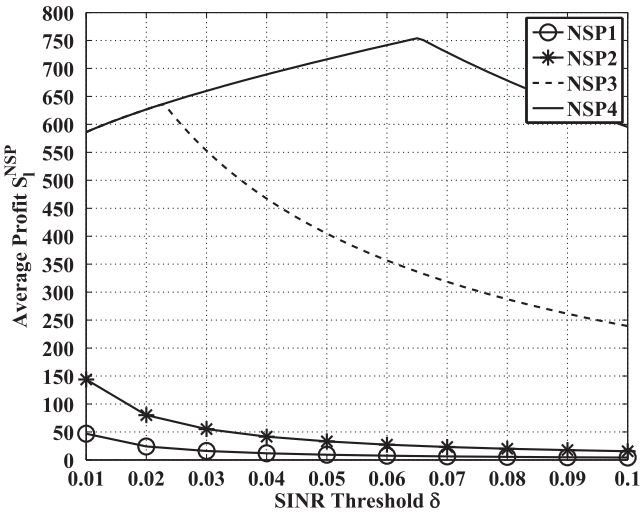

Fig. 5. Average profit of the four NSPs under different δ.

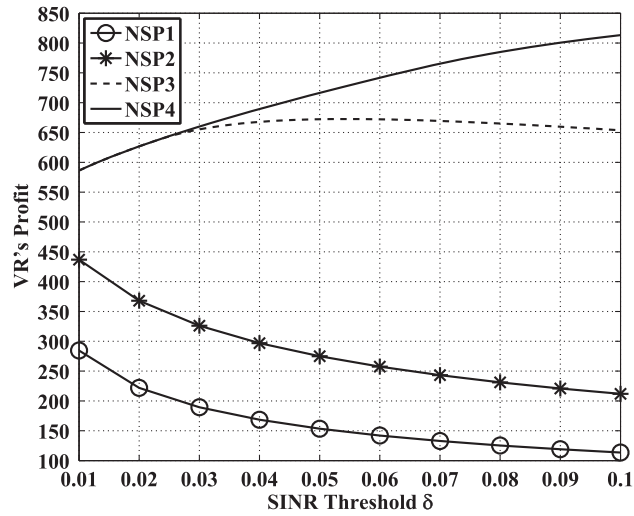

Fig. 6. VR's profit made from the four NSPs under different δ.

NSPs are the same in this region according to (17). Fig. 5 shows each NSP's average profit in (9) from the saved backhaul cost due to renting copies of the $F = 500$ videos, for which we set the file popularity parameter $\beta = 0.5$, and the file popularity is calculated according to (2). First, we can see that the NSP with more SBSs gains a larger profit. The profit for $\mathcal{L}_1$ with $\lambda_1 = 5$ is the lowest and close to zero. This is due to the high price charged $\mathcal{L}_1$ (see Fig. 4) and the low direct download probability $\Pr(\mathcal{E}_{1,f})$. Second, the profit of $\mathcal{L}_1$ and $\mathcal{L}_2$ are monotonically reducing with the increase in δ. This is because the downloading probabilities $\Pr(\mathcal{E}_{1,f})$ and $\Pr(\mathcal{E}_{2,f})$ reduce with the increase in δ. On the other hand, it is interesting to observe that the profit of $\mathcal{L}_3$ keeps increasing when $\delta < 0.023$, whereas it begins to reduce when $\delta \geq 0.023$. This is because when $\delta < 0.023$, $\mathcal{L}_3$ can increase the fraction $\tau_{3,f}$ to enhance its direct download probability $\Pr(\mathcal{E}_{3,f})$, thereby increasing its profit. However, $\tau_{3,f}$ reaches 1 when $\delta \geq 0.023$, and $\Pr(\mathcal{E}_{3,f})$ starts to reduce with the increase in δ. Hence, its profit drops with $\Pr(\mathcal{E}_{3,f})$. The profit of $\mathcal{L}_4$ can also be explained with the same reason.

Finally, we investigate VR's profit in (7) from renting video copies. Fig. 6 shows the VR's profit gained from each NSP. It is obvious that $\mathcal{L}_4$ contributes the most to the VR's profit. In the range of $0.01 \leq \delta \leq 0.1$, the contributions from $\mathcal{L}_1$ and $\mathcal{L}_2$ to the VR's profit

reduce with the growth of δ. The contribution from $\mathcal{L}_3$ to the VR's profit first increases and then slightly reduces with the growth of δ. The contribution from $\mathcal{L}_4$ to the VR's profit keeps increasing with δ. The reason behind these observations can be readily obtained from (7) combined with Figs. 3 and 4. Since the NSP $\mathcal{L}_4$ has the greatest density of SBSs, it will purchase the most video copies from the VR and have the highest probability of direct download. This explains why $\mathcal{L}_4$ contributes the most to the VR's profit, although the price on each video copy is the lowest for $\mathcal{L}_4$. Moreover, since $\tau_{4,f}$ keeps increasing until $\delta = 0.065$, as shown in Fig. 3, this explains why $\mathcal{L}_4$ has a dramatically increasing contribution to the VR's profit when $\delta \leq 0.065$ in Fig. 6. On the other hand, it is shown in Fig. 3 that $\tau_{1,f}$ and $\tau_{2,f}$ are fixed to one, regardless of the value of δ, and in Fig. 4 that the prices for $\mathcal{L}_1$ and $\mathcal{L}_2$ are decreasing with the increase in δ. This explains why the contributions from $\mathcal{L}_1$ and $\mathcal{L}_2$ to the VR's profit keep decreasing in Fig. 6.

VII. Conclusion

In this paper, we have considered a commercialized small-cell caching system consisting of a VR and multiple NSPs. In such a system, the VR leases its videos to the NSPs to gain profits, whereas the NSPs, after placing popular videos to their SBSs, can save the backhaul costs. We proposed a Stackelberg game-theoretic framework. by viewing the videos as a type of resources. We first modeled the MUs and SBSs as two independent PPPs via stochastic geometry and developed the probability of direct downloading. Then, based on the derived probability, we formulated the Stackelberg game to maximize the average profit of the VR and individual NSPs. Next, we investigated the SE via solving an optimization problem. Numerical results were provided to show that the proposed scheme is effective in pricing and resource allocation.

Appendix A
Proof of Theorem 1

Recall that the distribution of the SBSs owned by $\mathcal{L}_l$ that cache the video $\mathcal{F}_f$ is modeled as a "thinned" HPPP $\Phi_{l,f}$ with intensity $\tau_{l,f}\lambda_l$. We consider a typical MU $\mathcal{M}$ who wishes to connect to the nearest SBS $\mathcal{B}$ in $\Phi_{l,f}$. The event $\mathcal{E}_{l,f}$ represents that this SBS can provide $\mathcal{M}$ with an SINR no less than δ; thus, $\mathcal{M}$ can obtain the desired file from the cache of $\mathcal{B}$.

We conduct the analysis on $\Pr(\mathcal{E}_{l,f})$ for the typical MU $\mathcal{M}$ located at the origin. Since the network is interference dominant, we neglect the noise in the following. z denotes the distance between $\mathcal{M}$ and $\mathcal{B}$, x_Z denotes the location of $\mathcal{B}$, and $\rho(x_Z)$ denotes the received SINR at $\mathcal{M}$ from $\mathcal{B}$. Then, the average probability that $\mathcal{M}$ can download the video from $\mathcal{B}$ is shown in (19), at the bottom of the page, where we have

$$I \triangleq \sum_{x\in\{\Phi_1,\ldots,\Phi_L\}\setminus\{x_Z\}} h_x \|x\|^{-\alpha} \tag{20}$$

and the probability density function of z, i.e., $f_Z(z)$ is derived by the null probability of the HPPP $\Phi_{l,f}$ with the intensity of $\tau_{l,f}\lambda_l$. This null probability, i.e., the probability of the event $\mathcal{A}$ that there is no SBS in the area with radius of z is given by

$$\begin{aligned}\Pr(\mathcal{A}) &= e^{-\pi z^2 \tau_{l,f}\lambda_l} \frac{\left(\pi z^2 \tau_{l,f}\lambda_l\right)^0}{0!} \\ &= e^{-\pi z^2 \tau_{l,f}\lambda_l}.\end{aligned} \tag{21}$$

By using the derivative of (21), we can obtain $f_n(z) = 2\pi\tau_{l,f}\lambda_l z\exp(-\pi\tau_{l,f}\lambda_l z^2)$. The interference I consists of I_1 and I_2, where I_1 is emanating from the SBSs excluding those from $\Phi_{l,f}$, whereas I_2 is from the SBSs in $\Phi_{l,f}$ excluding $\mathcal{B}$. The SBSs contributing to I_1, denoted by $\Phi_{\overline{l,f}}$, have the intensity $(\sum_j^L \lambda_j - \tau_{l,f}\lambda_l)$, whereas those contributing to I_2 have the intensity $\tau_{l,f}\lambda_l$.

Similar to the PPP analysis in [12], we can obtain $\mathbb{E}_{I_1}(\exp(-z^\alpha\delta I_1))$ and $\mathbb{E}_{I_2}(\exp(-z^\alpha\delta I_2))$. By skipping the intermediate derivations, we finally reach

$$\begin{aligned}&\mathbb{E}_{I_1}\left(\exp\left(-z^\alpha\delta I_1\right)\right) \\ &= \exp\left(-\pi\left(\sum_j^L \lambda_j - \tau_{l,f}\lambda_l\right) C(\delta,\alpha) z^2\right)\end{aligned} \tag{22}$$

$$\begin{aligned}&\mathbb{E}_{I_2}\left(\exp(-z^\alpha\delta I_2)\right) \\ &= \exp\left(-\tau_{l,f}\lambda_l 2\pi \int_z^\infty \left(1 - \frac{1}{1+z^\alpha\delta r^{-\alpha}}\right) r dr\right) \\ &= \exp\left(-\tau_{l,f}\lambda_l \pi \delta^{\frac{2}{\alpha}} z^2 \frac{2}{\alpha} \int_{\delta^{-1}}^\infty \frac{x^{\frac{2}{\alpha}-1}}{1+x}\,\mathrm{d}x\right) \\ &= \exp\left(-\tau_{l,f}\lambda_l \pi \delta z^2 \frac{2}{\alpha-2}\, {}_2F_1\left(1, 1-\frac{2}{\alpha}; 2-\frac{2}{\alpha}; -\delta\right)\right)\end{aligned} \tag{23}$$

where we have

$$x \triangleq \delta^{-1} z^{-\alpha} r^\alpha. \tag{24}$$

$$\begin{aligned}\Pr\left(\rho(x_Z) \geq \delta\right) &= \int_0^\infty \Pr\left(\frac{h_{x_Z} z^{-\alpha}}{\sum_{l'\neq l}\sum_{x\in\Phi_{l'}} h_x\|x\|^{-\alpha} + \sum_{x\in\Phi_l\setminus x_Z} h_x\|x\|^{-\alpha}} \geq \delta \,\middle|\, z\right) f_Z(z)\mathrm{d}z \\ &= \int_0^\infty \Pr\left(h_{x_Z} \geq \frac{\delta\left(\sum_{x\in\{\Phi_1,\ldots,\Phi_L\}\setminus\{x_Z\}} h_x\|x\|^{-\alpha}\right)}{z^{-\alpha}} \,\middle|\, z\right) 2\pi\tau_{l,f}\lambda_l z\exp\left(-\pi\tau_{l,f}\lambda_l z^2\right)\,\mathrm{d}z \\ &= \int_0^\infty \mathbb{E}_I\left(\exp(-z^\alpha\delta I)\right) 2\pi\tau_{l,f}\lambda_l z\exp\left(-\pi\tau_{l,f}\lambda_l z^2\right)\,\mathrm{d}z\end{aligned} \tag{19}$$

By substituting (22) and (23) into (19), we have

$$\begin{aligned}&\Pr\left(\rho(x_Z)\geq\delta\right)\\&=\int_0^\infty \exp\left(-\pi\left(\sum_j^L\lambda_j-\tau_{l,f}\lambda_l\right)C(\delta,\alpha)z^2\right)\exp\\&\quad\times\left(-\pi\tau_{l,f}\lambda_l z^2A(\delta,\alpha)\right)2\pi\tau_{l,f}\lambda_l z\exp\left(-\pi\tau_{l,f}\lambda_l z^2\right)\mathrm{d}z\\&=\frac{\tau_{l,f}\lambda_l}{C(\delta,\alpha)\left(\sum_j^L\lambda_j-\tau_{l,f}\lambda_l\right)+A(\delta,\alpha)\tau_{l,f}\lambda_l+\tau_{l,f}\lambda_l}.\end{aligned}\quad(25)$$

■

REFERENCES

[1] N. Golrezaei, A. Molisch, A. Dimakis, and G. Caire, "Femtocaching and device-to-device collaboration: A new architecture for wireless video distribution," *IEEE Commun. Mag.*, vol. 51, no. 4, pp. 142–149, Apr. 2013.

[2] X. Wang, M. Chen, T. Taleb, A. Ksentini, and V. Leung, "Cache in the air: Exploiting content caching and delivery techniques for 5G systems," *IEEE Commun. Mag.*, vol. 52, no. 2, pp. 131–139, Feb. 2014.

[3] N. Golrezaei, P. Mansourifard, A. Molisch, and A. Dimakis, "Base-station assisted device-to-device communications for high-throughput wireless video networks," *IEEE Trans. Wireless Commun.*, vol. 13, no. 7, pp. 3665–3676, Jul. 2014.

[4] M. Ji, G. Caire, and A. F. Molisch, "Wireless device-to-device caching networks: Basic principles and system performance," *IEEE J. Sel. Areas Commun.*, vol. 34, no. 1, pp. 176–189, Jan. 2016.

[5] M. Ji, G. Caire, and A. Molisch, "Optimal throughput-outage trade-off in wireless one-hop caching networks," in *Proc. IEEE ISIT*, Jul. 2013, Istanbul, Turkey, pp. 1461–1465.

[6] A. Damnjanovic *et al.*, "A survey on 3GPP heterogeneous networks," *IEEE Wireless Commun.*, vol. 18, no. 3, pp. 10–21, Jun. 2011.

[7] M. Mirahmadi, A. Al-Dweik, and A. Shami, "Interference modeling and performance evaluation of heterogeneous cellular networks," *IEEE Trans. Commun.*, vol. 62, no. 6, pp. 2132–2144, Jun. 2014.

[8] M. Liebsch, S. Schmid, and J. Awano, "Reducing backhaul costs for mobile content delivery-An analytical study," in *Proc. IEEE ICC*, Ottawa, ON, Canada, Jun. 2012, pp. 2895–2900.

[9] K. Shanmugam, N. Golrezaei, A. Dimakis, A. Molisch, and G. Caire, "Femtocaching: Wireless content delivery through distributed caching helpers," *IEEE Trans. Inf. Theory*, vol. 59, no. 12, pp. 8402–8413, Dec. 2013.

[10] E. Bastug, M. Bennis, and M. Debbah, "Cache-enabled small cell networks: Modeling and tradeoffs," in *Proc. IEEE 11th ISWCS*, Barcelona, Spain, Aug. 2014, pp. 649–653.

[11] D. Stoyan, W. Kendall, and M. Mecke, *Stochastic Geometry and Its Applications*, 2nd ed. Chichester, U.K.: Wiley, 2003.

[12] M. Haenggi, J. Andrews, F. Baccelli, O. Dousse, and M. Franceschetti, "Stochastic geometry and random graphs for the analysis and design of wireless networks," *IEEE J. Sel. Areas Commun.*, vol. 27, no. 7, pp. 1029–1046, Sep. 2009.

[13] E. Altman, R. Marquez, R. El-Azouzi, D. Ros, and B. Tuffin, "Stackelberg approach for pricing differentiated services," in *Proc. 2nd Int. Conf. ValueTools*, 2007, Nantes, France, pp. 1–10.

[14] J. Pita, M. Jain, O. M. Tambe, S. Kraus, and R. Magori-cohen, "Effective solutions for real-world stackelberg games: When agents must deal with human uncertainties," in *Proc. 8th Int. Conf. AAMAS*, Budapest, Hungary, May 2009, pp. 369–376.

[15] G. Vazquez-Vilar, C. Mosquera, and S. Jayaweera, "Primary user enters the game: Performance of dynamic spectrum leasing in cognitive radio networks," *IEEE Trans. Wireless Commun.*, vol. 9, no. 12, pp. 3625–3629, Dec. 2010.

[16] A. Coluccia and E. Altman, "SINR base station placement and mobile association games under cooperation," in *Proc. IEEE 9th Annu. Conf. WONS*, Courmayeur, Italy, Jan. 2012, pp. 51–54.

[17] X. Kang, R. Zhang, and M. Motani, "Price-based resource allocation for spectrum-sharing femtocell networks: A Stackelberg game approach," *IEEE J. Sel. Areas Commun.*, vol. 30, no. 3, pp. 538–549, Apr. 2012.

[18] Q. Wang, W. Wang, S. Jin, H. Zhu, and N. Zhang, "Quality-optimized joint source selection and power control for wireless multimedia D2D communication using Stackelberg game," *IEEE Trans. Veh. Technol.*, vol. 64, no. 8, pp. 3755–3769, Aug. 2015.

[19] M. Cha, H. Kwak, P. Rodriguez, Y.-Y. Ahn, and S. Moon, "I tube, you tube, everybody tubes: Analyzing the world's largest user generated content video system," in *Proc. 7th ACM SIGCOMM Conf. Internet Meas.*, San Diego, CA, USA, 2007, pp. 1–14.

[20] H. Sarkissian, "The business case for caching in 4G LTE networks," Wireless 20/20, San Jose, CA, USA, Tech. Rep., 2014. [Online]. Available: http://www.wireless2020.com/docs/LSI_WP_Content_Cach_Cv3.pdf

A Low-Complexity Detection Algorithm for the Primary Synchronization Signal in LTE

Mohammad H. Nassralla,
Mohammad M. Mansour, *Senior Member, IEEE*, and
Louay M. A. Jalloul, *Senior Member, IEEE*

***Abstract*—One of the challenging tasks in Long-Term Evolution (LTE) baseband receiver design is synchronization, which determines the symbol boundary and transmitted frame start time and performs cell identification. Conventional algorithms are based on correlation methods that involve a large number of multiplications and, thus, lead to high receiver hardware complexity and power consumption. In this paper, a hardware-efficient synchronization algorithm for frame timing based on K-means clustering schemes is proposed. The algorithm reduces the complexity of the primary synchronization signal for LTE from 24 complex multiplications, which are currently best known in the literature, to just eight. Simulation results demonstrate that the proposed algorithm has negligible performance degradation with reduced complexity relative to conventional techniques.**

***Index Terms*—Correlation operation, K-means clustering, orthogonal frequency-division multiplexing (OFDM), primary synchronization signal, Third-Generation Partnership Project Long-Term Evolution (LTE).**

I. INTRODUCTION

The Third-Generation Partnership Project Long-Term Evolution (LTE) standard is based on orthogonal frequency-division multiple access (OFDMA) [1]. Upon call initiation, a search procedure performed by the user equipment (UE) is triggered to synchronize its receiver to the transmitting base station (known as eNodeB). During synchronization, the UE receiver acquires the frame starting position, symbol timing, carrier frequency offset, and cell identity information. While frame synchronization aims at detecting the beginning of each frame, it is not restricted to the initial call setup. The UE has to periodically search for neighboring cells for possible handovers. Moreover, due to the susceptibility of OFDMA systems to synchronization errors [2], the UE should always support a dynamic cell search procedure to update the frame timing and compensate for frequency offset, to sustain orthogonality among the subcarriers [1].

Manuscript received August 23, 2014; revised May 22, 2015, August 25, 2015; accepted November 23, 2015. Date of publication November 24, 2015; date of current version October 13, 2016. The review of this paper was coordinated by Prof. Y. Su.

M. H. Nassralla and M. M. Mansour are with the Department of Electrical and Computer Engineering, American University of Beirut, Beirut 1107 2020, Lebanon (e-mail: mmansour@ieee.org).

L. M. A. Jalloul is with Qualcomm Incorporated, San Jose, CA 95110 USA (e-mail: jalloul@ieee.org).

Color versions of one or more of the figures in this paper are available online at http://ieeexplore.ieee.org.

Digital Object Identifier 10.1109/TVT.2015.2503606